한국해양공학회 2001년도 추계학술대회 논문집 PP. 202~206

Simulation of Viscous Flow around the Moving Underwater Vehicle

SEUNG-HYUN KWAG*
*School of Mechanical Engineering, Halla University, Wonju 220-712, Korea

곽승현*
*한라대학교 기계공학부 산업기계시스템공학전공

KEY WORDS: Free Surface 자유표면, Viscous Flow 점성유동, Submerged Vehicle 잠수체, Navier-Stokes 나비에-스톡스, Third Derivative Upwind, 3차풍상미분, Wave Simulation 조파재연

ABSTRACT: *A three dimensional incompressible Navier-Stokes code based on the third derivative upwind is employed to simulate the flow around the underwater vehicle advancing on the calm water. Computations are carried out in the range of Froude numbers 0.4 to 0.7. The wave resistance, lift, moment and the pressure distribution on the body are calculated. Computations are performed in a rectangular grid system based on the Marker & Cell method. For validation, computation results are compared with existing experimental results.*

1. INTRODUCTION

The inviscid flow about a body of revolution has long since been formulated and studied in detail. Practically, because of the predominant viscous effect near the boundary layer, the related flow pattern is much more complicated, especially if the body is at an incidence with respect to the flow direction. The wake of the body becomes turbulent, and various types of cross flow separation takes place. The basic hull form of a modern submersible is typically a body of revolution. While maneuvering at high speed, the hull may be subject to severe hydrodynamic forces. Under certain conditions, the moment of forces about the center of buoyance of the body may cause instability. In order to achieve a higher envelope of maneuverability and controllability, the designers of the modern submersible have practical interest in predicting the hydrodynamic response for any given planned movement. Such interest can be best served by parallel efforts in enlarging the data base from controlled laboratory environment and developing accurate computational schemes. Extensive experiments were carried out by various research parties, some of the representative results were borrowed from references; Ramaprian(1981), Intermann(1986), and Kim(1991). More recently, computational efforts based on newly developed numerical schemes offer encouraging predictions; Vatsa(1989), Degani(1991), Hartwich(1990), Sung(1993), Meir (1985), Freeman(1932). This paper represents a study of the accuracy and feasibility of predicting forces and moment on a body of revolution hull form.

2. NUMERICAL SCHEME

2.1 Basic equations

Numerical simulations of 3-D free-surface flows are carried out by solving Navier-Stokes equations. The velocity components u, v and w at (n+1) time step are determined by

$$\begin{aligned} u^{n+1} &= (F^n - \Phi_x^n)\Delta t \\ v^{n+1} &= (G^n - \Phi_y^n)\Delta t \\ w^{n+1} &= (H^n - \Phi_z^n)\Delta t \end{aligned} \tag{1}$$

where

$$F^n = \frac{u^n}{\Delta t} + \left(\frac{1}{Re} + \nu_t\right)\nabla^2 u - \left(u^n\frac{\partial u}{\partial x} + v^n\frac{\partial u}{\partial y} + w^n\frac{\partial u}{\partial z}\right) - \frac{\partial}{\partial x}\left\{\nu_t\left(2\frac{\partial u}{\partial x}\right)\right\} - \frac{\partial}{\partial y}\left\{\nu_t\left(\frac{\partial u}{\partial y} + \frac{\partial v}{\partial x}\right)\right\} - \frac{\partial}{\partial z}\left\{\nu_t\left(\frac{\partial u}{\partial z} + \frac{\partial w}{\partial x}\right)\right\}$$

$$G^n = \frac{v^n}{\Delta t} + \left(\frac{1}{Re} + \nu_t\right)\nabla^2 v$$

$$-\left(u^n \frac{\partial v}{\partial x} + v^n \frac{\partial v}{\partial y} + w^n \frac{\partial v}{\partial z} \right)$$
$$-\frac{\partial}{\partial x}\left\{ \nu_t \left(\frac{\partial u}{\partial y} + \frac{\partial v}{\partial x} \right) \right\} - \frac{\partial}{\partial y}\left\{ \nu_t \left(2\frac{\partial v}{\partial y} \right) \right\}$$
$$-\frac{\partial}{\partial z}\left\{ \nu_t \left(\frac{\partial v}{\partial z} + \frac{\partial w}{\partial y} \right) \right\} \qquad (2)$$

$$H^n = \frac{w^n}{\Delta t} + \left(\frac{1}{Re} + \nu_t \right) \nabla^2 w$$
$$-\left(u^n \frac{\partial w}{\partial x} + v^n \frac{\partial w}{\partial y} + w^n \frac{\partial w}{\partial z} \right)$$
$$-\frac{\partial}{\partial x}\left\{ \nu_t \left(\frac{\partial u}{\partial z} + \frac{\partial w}{\partial x} \right) \right\} - \frac{\partial}{\partial y}\left\{ \nu_t \left(\frac{\partial v}{\partial z} + \frac{\partial w}{\partial y} \right) \right\}$$
$$-\frac{\partial}{\partial z}\left\{ \nu_t \left(2\frac{\partial w}{\partial z} \right) \right\}$$

and

$$\Phi^n = p + \frac{z}{Fn^2} \qquad (3)$$

$$\nabla^2 = \frac{\partial}{\partial x^2} + \frac{\partial}{\partial y^2} + \frac{\partial}{\partial z^2} \qquad (4)$$

Differentiating Eq. (1) with respect to x, y and z, we can get

$$\nabla^2 \Phi = F_x + G_y + H_z$$
$$-(u_x^{n+1} + v_y^{n+1} + w_z^{n+1}) / \Delta t \qquad (5)$$

The last term in Eq. (5) is expected to be zero to satisfy the continuity condition. Equation (5) can be solved by the relaxation method.

It is desirable to introduce coordinate transformations which simplify the computational domain in the transformed domain

$$\xi = \xi(x, y, z),\ \eta = \eta(x, y, z),\ \zeta = \zeta(x, y, z) \qquad (6)$$

Through transformations, Eq. (1) can be written,

$$q_t + U q_\xi + V q_\eta + W q_\zeta$$
$$= \left(\frac{1}{Re} + \nu_t \right) \nabla^2 q - K - REYSF(\xi, \eta, \zeta) \qquad (7)$$

where U, V and W are the contravariant velocities and K is the pressure gradient. The pressure is calculated by the following relaxation formula,

$$\Phi^{m+1} = \Phi^m + \omega \cdot (\Phi^{m+1} - \Phi^m) \qquad (8)$$

where (m+1) denotes the next time step and ω is a relaxation factor.

2.2 Computational procedure and boundary conditions

The N-S and Poisson equations are solved after transformation, in which the calculation proceeds through a sequence of loops each advancing the entire flow configuration through sufficiently small finite time increment. The output of each loop is taken as an initial condition for the next. The computation is performed until the state is steady. An Euler explicit scheme is used for the time marching procedure. Pressures are obtained throughout the fluid domain by solving the Poisson equation. Iterations are automatically stopped when the pressure difference between two consecutive approximations is smaller than a certain quantity ε, chosen a priori. The new pressure field generates a new velocity field. The velocity component is updated by using the time-forward difference form of the momentum equations.

The third order upstream difference is used for convection terms with the fourth-order truncation error, for example;

$$U \cdot (\delta f / \delta x)_{i,j,k}$$
$$= U_{i,j,k} \cdot (f_{i-2,j,k} - 8f_{i-1,j,k} + 8f_{i+1,j,k} - f_{i+2,j,k})/12 \qquad (9)$$
$$+ \left| U_{i,j,k} \right| \cdot (f_{i-2,j,k} - 4f_{i-1,j,k} + 6f_{i,j,k} - 4f_{i+1,j,k} + f_{i+2,j,k})/4$$

As boundary conditions, the following are used.

upstream

$u = 1,\ v = 0,\ w = 0$ and $p = 0$

$\Delta u = \Delta v = \Delta w = 0$

downstream

$u_\xi = v_\xi = w_\xi = 0$

$\Delta u_\xi = \Delta v_\xi = \Delta w_\xi = \Delta p_\xi = 0$

symmetrical

$u_\eta = v_\eta = w_\eta = 0$

$\Delta u_\eta = \Delta v_\eta = \Delta w_\eta = \Delta p_\eta = 0$

body surface

$u = v = w = 0,\ p_\zeta = 0$

$\Delta u = \Delta v = \Delta w = 0,\ \Delta p_\zeta = 0$

2.3 Free surface boundary condition

The fluid particle is moved on the free surface by

$$\frac{\partial h}{\partial t} + u\frac{\partial h}{\partial x} - w = 0 \Big|_{z=\zeta} \qquad (10)$$

The boundary condition for the free surface requires zero tangential stress and a normal stress that balances any externally applied normal stress. The displacement of the particle is given by

$$\Delta x = u \cdot \Delta t\ ,\quad \Delta h = w \cdot \Delta t \qquad (11)$$

where Δt is the time increment. On the other hand, the use of an Euler-type expression of the kinematic free surface boundary condition makes it possible to employ a higher finite difference scheme. The condition can be written as follows:

$$\frac{\partial h_i^{n+1}}{\partial t}+(u_i+\frac{\partial u_i}{\partial z}\Delta h_i)\cdot\frac{\partial h_i^{n+1}}{\partial x}-w_i=0 \tag{12}$$

where $h=h(x,t)$ represents the elevation.
Expanding in Taylor series, the derivative term can be discretized by using

$$\frac{\partial h_i^{n+1}}{\partial t}=\frac{1}{2\Delta t}\cdot(h^{n-1}-4h^n+3h^{n+1}) \tag{13}$$

For the $\partial h^{n+1}/\partial x$ derivative, the third order upwind difference(TOUD) is adopted.

$$c\frac{\partial h}{\partial x}=c\frac{1}{6\Delta x}(-2h_{i-3}+9h_{i-2}-18h_{i-1}+11h_i) \tag{14}$$

where c is the convective velocity; it can be decomposed into two parts. One is the central differencing term whose mathematical expression can be obtained by suitable Taylor expansions as follows:

$$\frac{c}{24\Delta x}(h_{i-3}-27h_{i-2}+27h_{i-1}-h_i) \tag{15}$$

The other is the diffusion term, which has the meaning of the fourth derivative of the velocity.

$$\frac{3c}{8\Delta x}(-h_{i-3}+7h_{i-2}-11h_{i-1}+5h_i) \tag{16}$$

The latter is expected to play a role to compensate the finiteness of the differentiation without phase shift. Here we similarly introduce the third derivative, Eq. (17) which contributes to reduce the phase shift together with damping. It is also obtained by the Taylor expansions around i -1½ as follows:

$$\frac{\alpha c}{(\Delta x)^3}(-h_{i-3}+3h_{i-2}-3h_{i-1}+h_i) \tag{17}$$

where $\alpha=-\frac{(\Delta x)^2}{6}$ is a constant.

Equation (17) is added to the right handed side term of Eq. (14), and the new formulation for the $\partial h/\partial x$ becomes,

$$c\frac{\partial h}{\partial x}=c\frac{1}{6\Delta x}(-h_{i-3}+6h_{i-2}-15h_{i-1}+10h_i)+\frac{\alpha c}{(\Delta x)^3}(-h_{i-3}+3h_{i-2}-3h_{i-1}+h_i) \tag{18}$$

Equation (18) is the same expression used by Dawson (1977) in his steady flow problem by the Rankine source method where he derived $\partial h/\partial x$ omitting the terms of the third derivatives intuitively. Introducing Eq. (13) and Eq. (18) into Eq. (12), the vertical coordinate increment at each time step can be,

$$\Delta h_i^n=\frac{3\Delta x(h_i^n-h_i^{n-1})+\Delta t\cdot[6w_i\Delta x+u_i(\Delta h_{i-3}^n-6\Delta h_{i-2}^n+15\Delta h_{i-1}^n-Q_i^n)]}{9\Delta x+\Delta t\cdot[10u_i+Q_i^n\frac{\partial u}{\partial z}-6\Delta x\frac{\partial w}{\partial z}]} \tag{19}$$

The expression is of the second order accuracy for $h(0(h^2))$ for any $u>0$. $Q^n{}_i$ in Eq. (19) is

$$Q_i^n=-h_{i-3}^n+6h_{i-2}^n-15h_{i-1}^n+10h_i^n \tag{20}$$

where h at the $(n+1)^{th}$ step is calculated as

$$h^{n+1}=h^n+\Delta h^n \tag{21}$$

3. RESULTS AND DISCUSSION

3.1 Underwater Body of Revolution

The underwater body of revolution was numerically tested at Froude number of 0.4 to 0.7. Figure 1(a) shows the sectional grid view where the grid size is 104x48x23. Figure 1(b) is the grid for the revolutional body at incidence. The time increment Δt is 0.0005 to meet the Courant condition. The Baldwin-Lomax model is used for the turbulence.

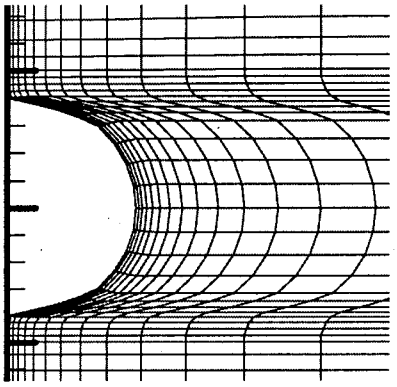

Fig. 1(a) Sectional view of grid generation

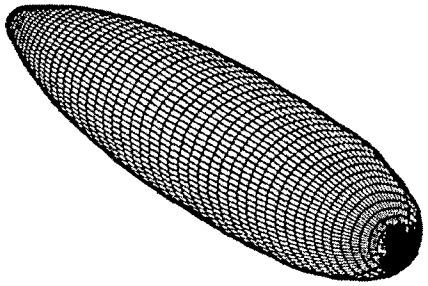

Fig. 1(b) Grid view of revolutional body

For the computation domain, 80% of the vehicle length is occupied in lateral direction, and two and half times in downstream. The grid is made as H-H topology to treat the free surface movement more conveniently. The wave height contours are shown in Fig. 2 at two different Froude numbers.

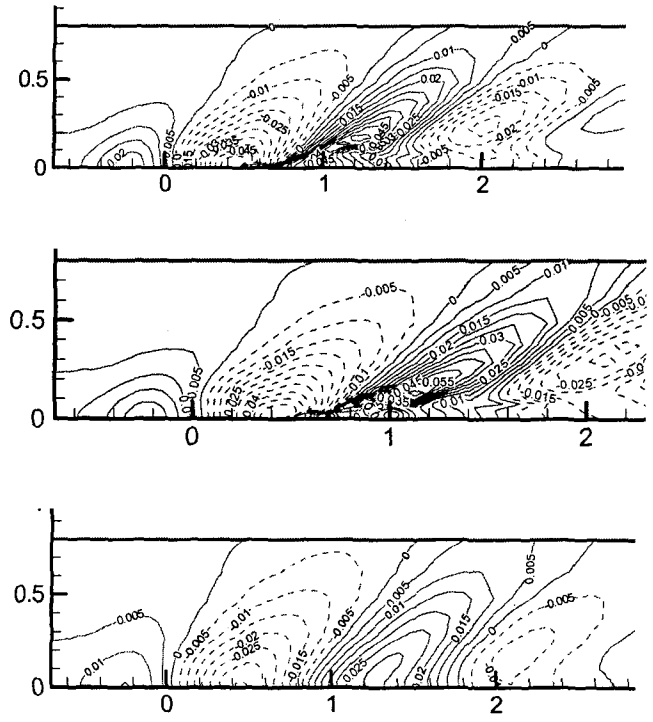

Fig. 2 Free surface waves (upper: d/h=0.16, t=3.0
middle: d/h=0.16, t=4.0, lower: d/h=0.245, t=3.0)

In Fig. 3, the velocity vectors can be seen at three sections; near near the bow, midship and near the stern at d/h= 0.16. Fig. 4 shows the comparison of the hydrodynamic coefficients at different Froude numbers. The present results agree well with others.

Fig. 5 shows the lift, drag and moment acting on the spheroid as a function of time. As seen, the solution is close to the steady state after the body has moved three body lengths.

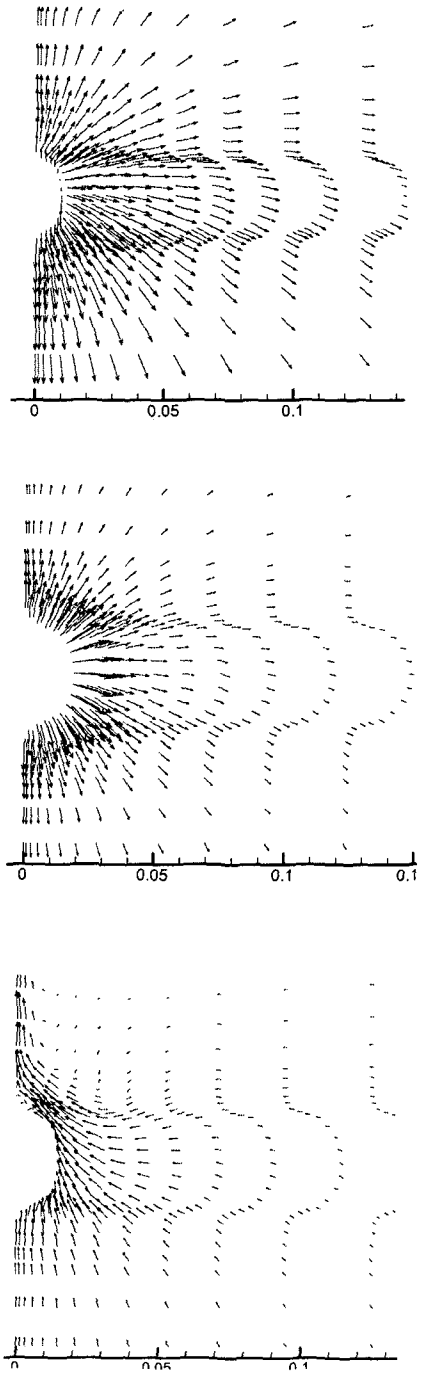

Fig. 3 Velocity vectors at d/h=0.16 (upper: near the bow, middle: midship, lower: near the stern)

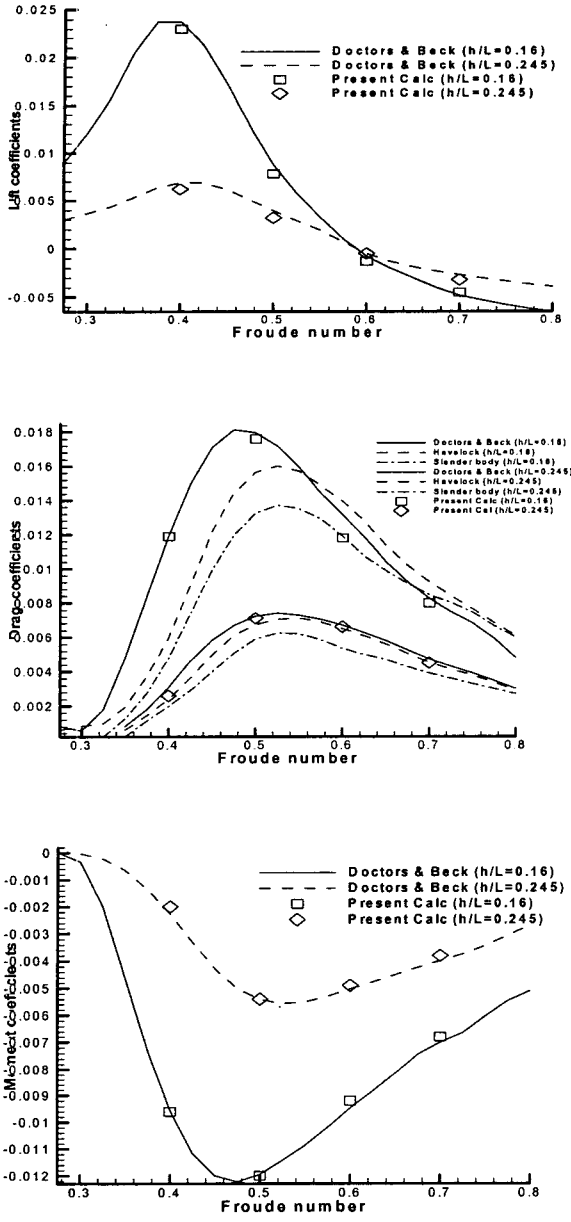

Fig. 4 Hydrodynamic coefficients at different Froude numbers

4. CONCLUSION

For the underwater vehicle, the flow characteristics is numerically investigated by showing the wave patterns on the free surface. Hydrodynamic coefficients are compared at different Froude numbers. The calculated results agree well with others' results. The lift, drag and moment are shown as a function of time. The solution shows the steady state after the body has moved several body lengths.

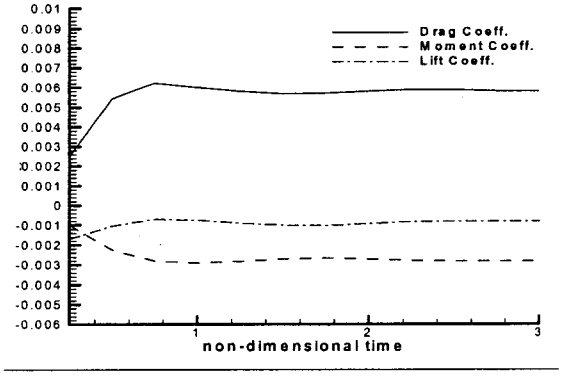

Fig. 5 Hydrodynamic coefficients along the time marching

REFERENCES

Dawson, C. W. (1977), "A practical Computer Method for Solving Ship Wave Problems," Proc. 2nd Int. Conf. on Num. Hydro., U. of California, Berkeley, pp. 30-38

Degani, D., Schiff, L. B. and Levy, Y., (1991), "Numerical prediction of Subsonic Turbulent Flow over Slender Bodies at High Incidence", AIAA Jour., Vol. 29, No. 12, pp. 2054-2061

Freeman, H. B. (1932), "Force Measurements on a 1/40 Scale Model of the U.S. Airship Akron," T. R. No. 432, NACA

Hartwich, P. M., Hall, R. M. (1990), "Navier-Stokes Solution for Vortical Flow over a Tangent-Ogive Cylinder", AIAA Jour., Vol. 28, No. 7, pp. 1171-1179

Intermann, G. A. (1986). "Experimental Investigation of the location and Mechanism of Local Flow Separation on a 3 Caliber Tangent Ogive Cylinder at Moderate Angles of Attack", M.S. Thesis, Univ. of Florida, Gainesville, FL

Kim, S. E., Patel V. C. (1991). "Separation on a Spheroid at Incidence: Turbulent Flow", Second Int. Colloquium on Viscous FLuid Dynamics in Ship and Ocean Technology, Osaka

Meir, H. V., Cebeci, T. (1985), "Flow Characteristic of a Revolution at Incidence", 3rd Symp. on Numerical and Physical Aspects of Aerodynamic Flows, California

Ramaprian, B. R., Patel, V. C. and Choi, D. H. (1981). "Mean flow Measurements in the Three Dimensional Boundary Layer over a Body of Revolution at Incidence", Jour. Fluid Mech., Vol. 103, pp. 479-504

Sung, C. H., Griffin, M. J., Ysai, J. F. and Huang, T. T. (1993), "Incompressible Flow Computation of Force and Moments on Bodies of Revolution an Incidence", AIAA-93-0787, 31st Aerospace Science Meeting and Exhibit, NV

Vasta, V. N., Thomas J. L. and Wedan, B. W. (1989), "Navier-Stokes Computations of Prolate at Angle of Attack", AIAA Jour.. Vol. 26, No. 11, pp. 986-993